

# Ergodicity properties of quantum expectation values in entangled states

C. Sudheesh\*

*Theoretical Physics Division, Physical Research Laboratory, Ahmedabad 380 009, India*

S. Lakshmibala<sup>†</sup> and V. Balakrishnan<sup>‡</sup>

*Department of Physics, Indian Institute of Technology-Madras, Chennai 600 036, India*

(Dated: February 1, 2008)

Using a model Hamiltonian for a single-mode electromagnetic field interacting with a nonlinear medium, we show that quantum expectation values of subsystem observables can exhibit remarkably diverse ergodic properties even when the dynamics of the total system is regular. The time series of the mean photon number is studied over a range of values of the ratio of the strength  $\gamma$  of the nonlinearity to that of the inter-mode coupling  $g$ . We obtain the power spectrum, estimate the embedding dimension of the reconstructed phase space and the maximal Liapunov exponent  $\lambda_{\max}$ , and find the recurrence-time distribution of the coarse-grained dynamics. The dynamical behavior ranges from quasiperiodicity (for  $\gamma/g \ll 1$ ) to chaos as characterized by  $\lambda_{\max} > 0$  (for  $\gamma/g \gtrsim 1$ ), and is interpreted.

PACS numbers: 05.45.Mt, 42.50.-p, 42.50.Dv, 42.50.Md

Classical nonlinear dynamical systems generically exhibit a long-time behavior that is ergodic—either on the energy surface (in Hamiltonian systems) or on some attractor (in dissipative systems). A hierarchy of randomness can be identified, ranging from ergodicity to global exponential sensitivity to initial conditions. Quantum systems, on the other hand, are governed by linear equations (the Schrödinger equation for the state vector or the Liouville equation for the density operator). The randomness in a quantum system, and the precise manner in which its information content changes with time, are not easily determined.

At least two different approaches have been employed in identifying signatures of the ergodicity properties of the quantum counterpart of a generic classical system [1]. One of these relies on the observation that such signatures are manifested in the energy-level statistics of the corresponding quantum system. If the system is classically integrable, the quantum levels cluster together, and could even cross when a specific parameter in the Hamiltonian is varied [2]. A classically chaotic system, on the other hand, has its corresponding quantum levels so correlated as to resist such crossings [3]. Another approach is based on the dynamics of the overlap between two quantum states of the same physical system which originate from the same initial state, but with slightly different values of one of the control parameters [4]. The time-dependent overlap is close to unity for all  $t$  if the normalized initial state is located in a regular region of the classical phase space. In contrast, if the initial state is in a chaotic region of this space, the overlap falls off exponentially in time.

These lines of investigation concern quantum signatures of classical dynamics. The inverse problem is of importance, and has also received attention: namely, the identification of signatures of non-classical effects such as

wave packet revivals in the temporal behavior of quantum expectation values (which, in turn, could be regarded as effective dynamical variables in an appropriate ‘phase space’). (A (near-)revival of an initial state  $|\psi(0)\rangle$  at  $t = T_{\text{rev}}$  implies that  $|\langle\psi(0)|\psi(T_{\text{rev}})\rangle|^2 \simeq 1$ .) The dynamics of a single mode of the radiation field governed by a nonlinear quantum Hamiltonian  $H$  enables us to understand the connections between the behavior of quantum expectation values and various non-classical effects displayed in wave packet dynamics [5].

In order to explore more thoroughly the range of dynamical behavior of expectation values of observables, in particular in the presence of entanglement, we need a system in which revival phenomena can either occur or be suppressed, depending on the values of the parameters in  $H$ . An uncomplicated but nontrivial  $H$  for our purposes is the one that describes the interaction of a single-mode field of frequency  $\omega$  with the atoms of the nonlinear medium through which it propagates. The medium is modeled [6] by an anharmonic oscillator with frequency  $\omega_0$  and nonlinearity parameter  $\gamma$ . The Hamiltonian of the total system is given by

$$H = \hbar\omega a^\dagger a + \hbar\omega_0 b^\dagger b + \hbar\gamma b^{\dagger 2} b^2 + \hbar g (a^\dagger b + b^\dagger a). \quad (1)$$

$(a, a^\dagger)$  are the field annihilation and creation operators,  $(b, b^\dagger)$  are the corresponding atomic oscillator operators, and  $g$  quantifies the coupling between the field and atom modes. Importantly, although the photon number operator  $N = a^\dagger a$  does not commute with  $H$  for any  $g \neq 0$ , the *total* number operator  $N^{\text{tot}} = (a^\dagger a + b^\dagger b)$  does so for all values of the parameters in  $H$ . While this implies that  $H$  can be cast in block-diagonal form in a direct-product basis of field and atom Fock states, the model is not trivial. A simple way to see this is to re-write  $H$  in terms of spin operators  $J_i$  ( $i = 1, 2, 3$ ) constructed from the two pairs of boson operators  $(a, a^\dagger)$  and  $(b, b^\dagger)$ . It is

then easily seen that the system of Heisenberg equations of motion for the spin operators does not close.

The quantum mechanical expectation value  $\langle N(t) \rangle$  (or the mean energy of the field mode) serves as a very convenient variable to probe the dynamics of this subsystem. It varies with time because of the coupling between the two modes, and it deviates from periodicity because of the nonlinearity in  $H$ . Its temporal behavior is remarkably diverse, ranging from quasiperiodic to chaotic, depending strongly on the initial state and the parameter regime—in particular, on the degree of coherence of the initial state, and on the ratio  $\gamma/g$  of the strengths of the nonlinearity and the field-atom coupling. We have studied the dynamics for states that are initially non-entangled direct products of the field and atomic oscillator states: specifically, states with the field in a coherent state  $|\alpha\rangle$  (CS) or an  $m$ -photon-added coherent state  $|\alpha, m\rangle$  (PACS), while the atomic oscillator is in its ground state  $|0\rangle$ . Recall that the CS  $|\alpha\rangle$  ( $\alpha \in \mathbb{C}$ ) satisfies  $a|\alpha\rangle = \alpha|\alpha\rangle$ , and is a minimum uncertainty state. The normalized PACS is defined [7] as  $|\alpha, m\rangle = (a^\dagger)^m |\alpha\rangle / [m! L_m(-\nu)]^{1/2}$  where  $m$  is a positive integer,  $\nu = |\alpha|^2$ , and  $L_m$  is the Laguerre polynomial of order  $m$ . A PACS possesses the useful properties of quantifiable and tunable degrees of departure from perfect coherence and Poissonian photon statistics. For brevity, we write  $|\alpha\rangle \otimes |0\rangle = |\alpha; 0\rangle$  and  $|\alpha, m\rangle \otimes |0\rangle = |(\alpha, m); 0\rangle$  for the initial states considered.  $\langle N(0) \rangle = \nu$  and  $[(m+1)L_{m+1}(-\nu)/L_m(-\nu)] - 1$ , respectively, in the two cases.

We have carried out a detailed analysis of the time series (using a time step  $\delta t$  ranging from  $10^{-2}$  for small  $\gamma/g$  to  $10^{-1}$  for large  $\gamma/g$ ) generated by the values of the mean photon number  $\langle N(t) \rangle$  computed over long intervals of time ( $10^6$  time steps), including phase space reconstruction, estimation of the minimum embedding dimension  $d_{\text{emb}}$ , calculation of the power spectrum [8, 9, 10], and recurrence-time statistics (using time series of  $10^7$  steps when necessary). We use a robust algorithm [11] developed for the estimation of the maximal Liapunov exponent  $\lambda_{\text{max}}$  from data sets represented by time series (see also [12]). The phase-space reconstruction procedure (including the extraction of  $d_{\text{emb}}$ ) has been carried out carefully, and it has been checked that any further increase in the dimensionality of the reconstructed phase space does not alter the inferences made regarding the exponential instability, if any, of the system.

For small values ( $\ll 1$ ) of  $\gamma/g$ , near-revivals and fractional revivals of the initial state occur, that are manifested in the entropy of entanglement of the system [13]. Correspondingly, we find that the dynamics of  $\langle N(t) \rangle$  ranges from periodicity to ergodicity, but is not chaotic, essentially independent of the nature of  $|\psi(0)\rangle$ . As a case representative of weak nonlinearity, we have chosen the parameter values  $\gamma = 1$ ,  $g = 100$ . Figure 1 (a), a log-linear plot of the power spectrum  $S(f)$  (the Fourier transform of the autocorrelation computed from the time

series of  $\langle N(t) \rangle$ ) as a function of the frequency  $f$  when  $|\psi(0)\rangle = |\alpha; 0\rangle$ , is indicative of quasiperiodic behavior. With increasing lack of coherence of the initial field state, the number of frequencies seen in  $S(f)$  increases. This is already evident from Fig. 1 (b), which corresponds to  $|\psi(0)\rangle = |(\alpha, 5); 0\rangle$ .

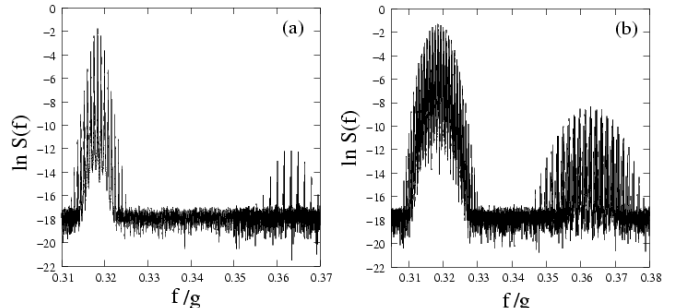


FIG. 1: Power spectrum of the mean photon number *vs.* the frequency (in units of  $g$ ) for the initial states (a)  $|\alpha; 0\rangle$  and (b)  $|(\alpha, 5); 0\rangle$  with  $\gamma/g = 10^{-2}$  and  $\nu = 1$ .

In contrast to the case of weak nonlinearity, the nature of the subsystem dynamics changes drastically when  $\gamma/g \gtrsim 1$ . As representative values for this nonlinearity-dominated regime, we have set  $\gamma = 5$ ,  $g = 1$ . We first examine the case corresponding to  $\nu = 1$ . For an initial field CS, both the time series and  $S(f)$  confirm that the subsystem dynamics is not chaotic. In contrast to this, an initial PACS leads to a chaotic form for  $S(f)$ , for sufficiently large values of  $m$ . This is supported by an estimation of  $\lambda_{\text{max}}$  from the time series. The initial set of separations between the  $j^{\text{th}}$  pair of nearest neighbors in the reconstructed phase space evolves to the set  $\{d_j(k)\}$  after  $k$  time steps. Then  $\lambda_{\text{max}}$  is the slope of the plot of  $\langle \ln d_j(k) \rangle$  (the average is over all values of  $j$ ) against  $t$  in the linear region lying in between the initial transient and final saturation regions. Figure 2 (a) depicts  $\langle \ln d_j(k) \rangle$  *vs.*  $t$  for  $|\psi(0)\rangle = |(\alpha, 5); 0\rangle$ , and the estimate of  $\lambda_{\text{max}}$ , whose positivity indicates a chaotic variation of the mean energy of the field mode. For a given value of  $\gamma/g$ , an increase in  $\nu$  leads to chaotic behavior even for an initial coherent field state. This is demonstrated in Fig. 2 (b), which shows  $\langle \ln d_j(k) \rangle$  *vs.*  $t$  for  $|\psi(0)\rangle = |\alpha; 0\rangle$  with  $\nu = 10$ . We further find that  $\lambda_{\text{max}}$  increases systematically with  $m$  for an initial PACS.

Table 1 summarizes these conclusions. In order to rule out round-off or truncation errors as the source of the computed chaotic behavior, we have verified in each case that the conclusions are not altered if  $\langle b^\dagger b \rangle$  is chosen as the signal for which the time-series data is computed, and that  $\langle N \rangle + \langle b^\dagger b \rangle$  does remain constant, as required. The entropy of entanglement (not presented here) provides independent corroboration of the dynamical behavior as deduced from  $S(f)$  and  $\lambda_{\text{max}}$ .

Our conclusions are reinforced by a detailed analysis

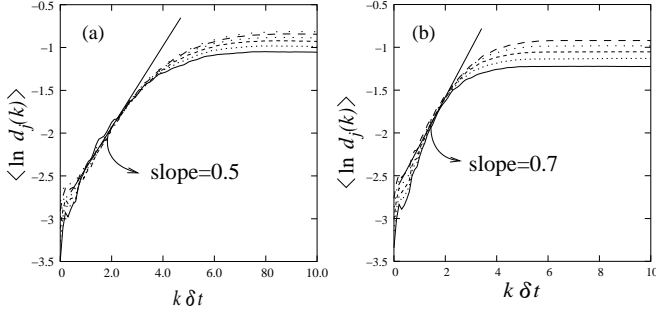


FIG. 2:  $\langle \ln d_j(k) \rangle$  vs.  $t$  for the initial states (a)  $|(\alpha, 5); 0\rangle$  with  $\gamma/g = 5$  and  $\nu = 1$  and (b)  $|\alpha; 0\rangle$  with  $\gamma/g = 5$  and  $\nu = 10$ . The solid line corresponds to an embedding dimension  $d_{\text{emb}} = 5$ , and the dotted lines to values of  $d_{\text{emb}}$  from 6 to 10.

		Increasing departure from coherence $\longrightarrow$		
		Initial state		
		$ \alpha; 0\rangle$	$ (\alpha, 1); 0\rangle$	$ (\alpha, 5); 0\rangle$
Increasing nonlinearity $\downarrow$	$\gamma/g=10^{-2}$ $ \alpha ^2=\nu=1$	regular	regular	regular
	$\gamma/g=10^{-2}$ $\nu=5$	regular	regular	regular
	$\gamma/g=5$ $\nu=1$	regular	regular	chaotic $\lambda_{\text{max}} \approx 0.5$
	$\gamma/g=5$ $\nu=5$	chaotic $\lambda_{\text{max}} \approx 0.6$	chaotic $\lambda_{\text{max}} \approx 0.7$	chaotic $\lambda_{\text{max}} \approx 0.9$
	$\gamma/g=5$ $\nu=10$	chaotic $\lambda_{\text{max}} \approx 0.7$	chaotic $\lambda_{\text{max}} \approx 0.8$	chaotic $\lambda_{\text{max}} \approx 1.0$

Table 1: Qualitative dynamical behavior of the mean photon number of a single-mode electromagnetic field interacting with a nonlinear medium. “Regular”  $\Rightarrow \lambda_{\text{max}} = 0$ .

of another important characterizer of dynamical behavior: recurrence statistics of the coarse-grained dynamics of  $\langle N(t) \rangle$  as represented by its time series. For the range of parameter values we use, the scatter in  $\langle N(t) \rangle$  is typically  $\gtrsim 1$ . We use a cell size  $\sim 10^{-2}$  and very long time series. This enables us to numerically construct the invariant density  $\rho$  (and hence the stationary measure  $\mu$  for any cell  $C$ ), as well as the distribution  $F(\tau)$  of the time  $\tau$  of first recurrence or return to  $C$ . The mean recurrence time  $\langle \tau \rangle$  can then be calculated, and compared with the result  $\langle \tau \rangle = \mu^{-1}$  that follows from the Poincaré recurrence theorem.[14]. As the latter is derived from the requirement of ergodicity alone, an agreement between the two values confirms that the dynamics is indeed ergodic in all the cases studied. We present here just two representative cases, both of which are also included in Table 1, for ready reference. The first corresponds to weak nonlinearity ( $\gamma/g = 10^{-2}$ ) and

$|\psi(0)\rangle = |(\alpha, 1); 0\rangle$ ,  $\nu = 1$ . According to Table 1, this case is non-chaotic. Figure 3 (a) shows the invariant den-

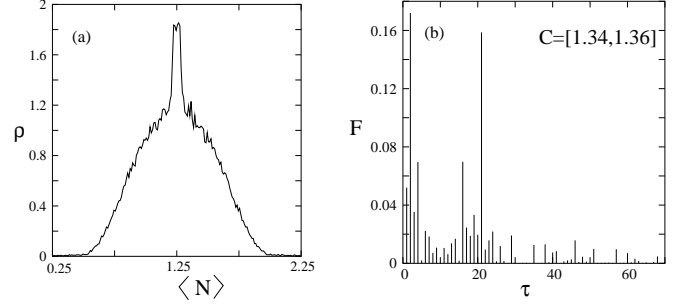


FIG. 3: (a) Invariant density and (b) first-recurrence-time distribution for the cell  $C$  from the time series of  $\langle N(t) \rangle$ , for weak nonlinearity.  $F(\tau)$  is characteristic of quasiperiodic dynamics.

sity, while (b) shows the actual recurrence time distribution. The discrete nature of the latter is a clear indication that the dynamics is actually quasiperiodic [15]. In marked contrast, consider a case of strong nonlinearity,  $\gamma/g = 5$  and  $|\psi(0)\rangle = |(\alpha, 1); 0\rangle$ ,  $\nu = 10$ . According to Table 1, this case is chaotic, with  $\lambda_{\text{max}} = 0.80$ . Figure

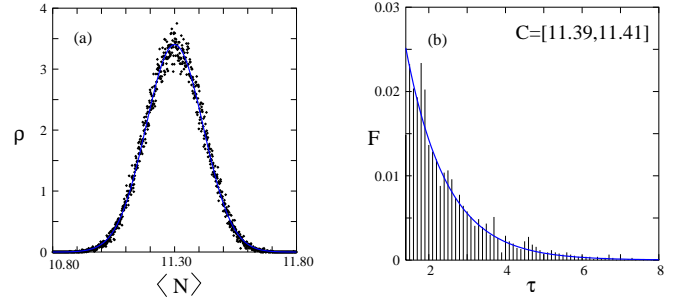


FIG. 4: (a) Invariant density and (b) first-recurrence-time distribution for the cell  $C$  from the time series of  $\langle N(t) \rangle$ , for strong nonlinearity.  $F(\tau)$  is characteristic of chaotic dynamics.

4 (a) shows that the invariant density is in fact well-approximated by a Gaussian in this case. More importantly,  $F(\tau)$  is very well fitted by the exponential distribution  $\mu e^{-\mu\tau}$ . This is precisely the distribution expected in a hyperbolic dynamical system, for a sufficiently small cell size [16]. Moreover, in such a system successive recurrences to a cell must be uncorrelated and Poisson-distributed. We have further confirmed this feature by examining the distribution of two successive recurrences, using even longer time series ( $10^7$  steps). The distribution is again well fitted by the next term in the Poisson distribution,  $\mu^2 \tau e^{-\mu\tau}$ .

Now consider the completely *classical* counterpart of the Hamiltonian in Eq. (1). Let the linear harmonic oscillator associated with  $(a, a^\dagger)$  have a mass  $m$ , position

$x$  and momentum  $p_x$ , and let that associated with  $(b, b^\dagger)$  have a mass  $M$ , position  $y$  and momentum  $p_y$ . Putting in all the constant factors (including  $\hbar$ ) in the definitions of the raising and lowering operators in Eq. (1), we get  $H(x, p_x, y, p_y)$ . When  $\hbar \rightarrow 0$ , the only consistent way to obtain a non-trivial, finite expression for the classical Hamiltonian  $H_{cl}$  is to let  $\gamma \rightarrow 0$  simultaneously, such that the ratio  $\gamma/\hbar \rightarrow \lambda = \text{a finite number}$ . Then, with  $H_1 = p_x^2/(2m) + m\omega^2 x^2/2$  and  $H_2 = p_y^2/(2M) + M\omega_0^2 y^2/2$ , we find

$$H_{cl} = H_1 + H_2 + (\lambda/\omega_0^2) H_2^2 + (g/\sqrt{\omega\omega_0}) \left( \sqrt{mM} \omega\omega_0 xy + p_x p_y / \sqrt{mM} \right). \quad (2)$$

The counterpart of  $N^{\text{tot}}$  is  $N_{cl}^{\text{tot}} = H_1/\omega + H_2/\omega_0$ , which Poisson-commutes with  $H_{cl}$ . Hence the 2-freedom classical system is Liouville-Arnold integrable. Further, although  $H_{cl}$  has cross terms that could change sign,  $N_{cl}^{\text{tot}} = \text{constant}$  is a hyperellipsoid in the 4-dimensional phase space, so that the motion is bounded for any set of initial conditions. All four Liapunov exponents vanish, and the classical motion is always regular, and restricted to a 2-torus, for each set of initial conditions. This behavior is indeed very different from the much more diverse one found for the quantum expectation value  $\langle N(t) \rangle$ .

What, then, is the interpretation of a positive value for  $\lambda_{\text{max}}$ , and the hyperbolicity implied by the recurrence-time statistics, as deduced from the time series for the subsystem variable  $\langle N \rangle$  (equivalently,  $\langle b^\dagger b \rangle$ ) in the quantum mechanical case? To start with, we note that a comparison of the quantum and classical cases is not always straightforward[17], and the case at hand is one such instance. Letting  $\gamma \rightarrow 0$  would remove the nonlinear term  $b^{\dagger 2} b^2$  in the quantum  $H$ . In that case the dynamics of  $\langle N(t) \rangle$  reduces to a trivial periodic exchange of energy between the field and atom modes. The origin of this dichotomy can be traced back to the inadequacy of the naive Ehrenfest theorem, which does not generally take into account the non-commutativity between  $x$  and  $p$ , in retrieving the classical regime of the quantum system. An outcome of this feature is that the Liapunov exponents that characterize the dynamical behavior of classical and quantum expectation values of the same observable can indeed be very different from each other [18]. The following observation [19] is pertinent in this regard. In isolated quantum systems with a discrete energy spectrum, using unitarity and the Schwarz inequality, it can be established that the Liapunov exponents would vanish, if computed from time-series data collected over a sufficiently long time (which could be much longer than the characteristic time scales in the problem), indicative of non-chaotic behavior. However, once measurement upon the system is included through appropriate interaction with an external system, the corresponding Liapunov exponents need not vanish. In the present context, the interaction between the modes is ef-

fectively tantamount to continual measurement upon either subsystem. Hence the dynamics of a subsystem, as deduced from time-series data of the corresponding variables, may show chaotic behavior, even if the system as a whole does not. The exponential instability associated with a positive Liapunov exponent is indicative of the manner in which an initial wave packet spreads, and the entanglement of the system increases, under time evolution. These aspects are worth bearing in mind, inasmuch as systems are ultimately quantum mechanical, and measured data are generically the time series of observables.

This work was supported in part by Project No. SP/S2/K-14/2000 of the Department of Science and Technology, India.

---

\* Electronic address: sudheesh@prl.res.in

† Electronic address: slbala@physics.iitm.ac.in

‡ Electronic address: vbalki@physics.iitm.ac.in

- [1] F. Haake, *Quantum Signatures of Chaos* (Springer-Verlag, Berlin, 1991).
- [2] M. V. Berry and M. Tabor, Proc. R. Soc. Lond. A **356**, 375 (1977).
- [3] M. V. Berry and M. Tabor, Proc. R. Soc. Lond. A **349**, 101 (1976); M. V. Berry, in *Chaotic Behavior of Deterministic Systems*, Editors G. Iooss, R. H. G. Helleman, and R. Stora, Les Houches Session XXXVI (1981) (North-Holland, Amsterdam, 1983).
- [4] A. Peres, Phys. Rev. A **30**, 1610 (1984).
- [5] C. Sudheesh, S. Lakshmibala, and V. Balakrishnan, Phys. Lett. A **329**, 14 (2004); Europhys. Lett. **71**, 744 (2005); J. Opt. B: Quant. Semiclass. Opt. **7**, S728 (2005).
- [6] G. S. Agarwal and R. R. Puri, Phys. Rev. A **39**, 2969 (1989).
- [7] G. S. Agarwal and K. Tara, Phys. Rev. A **43**, 492 (1991).
- [8] H. D. I. Abarbanel, *Analysis of Observed Chaotic Data* (Springer-Verlag, New York, 1995).
- [9] P. Grassberger and I. Procaccia, Phys. Rev. Lett. **50**, 346 (1983).
- [10] A. M. Fraser and H. L. Swinney, Phys. Rev. A **33**, 1134 (1986).
- [11] M. T. Rosenstein, J. J. Collins, and C. J. De Luca, Physica D **65**, 117 (1993).
- [12] H. Kantz, Phys. Lett. A **185**, 77 (1994).
- [13] C. Sudheesh, S. Lakshmibala, and V. Balakrishnan, J. Phys. B: At. Mol. Opt. Phys. **39**, 3345 (2006).
- [14] M. Kac, *Probability and Related Topics in Physical Sciences* (Interscience, New York, 1959).
- [15] M. Theunissen, C. Nicolis, and G. Nicolis, J. Stat. Phys. **94**, 437 (1999); S. Seshadri, S. Lakshmibala, and V. Balakrishnan, Phys. Lett. A **256**, 15 (1999).
- [16] M. Hirata, Ergod. Th. Dyn. Systems **13**, 533 (1993); V. Balakrishnan and M. Theunissen, Stoch. Dyn. **1**, 339 (2001).
- [17] R. G. Littlejohn, Phys. Rep. **138**, 193 (1986).
- [18] L. E. Ballentine, Y. Yang, and J. P. Zibin, Phys. Rev. A **50**, 2854 (1994).
- [19] S. Habib, K. Jacobs, and K. Shizume, Phys. Rev. Lett. **96**, 010403 (2006).